Eur. Phys. J. B **68**, 523–527 (2009)
DOI: 10.1140/epjb/e2009-00115-6

THE EUROPEAN PHYSICAL JOURNAL B

Regular Article

Fast initial qubit dephasing and the influence of substrate dimensions on error correction rates

R. Doll[1], P. Hänggi[1], S. Kohler[1], and M. Wubs[2,a]

[1] Institut für Physik, Universität Augsburg, Universitätsstraße 1, 86135 Augsburg, Germany
[2] Niels Bohr International Academy & QUANTOP, The Niels Bohr Institute, Copenhagen University, 2100 Ø, Denmark

Received 22 December 2008
Published online 1st April 2009 –

Abstract. Keeping single-qubit quantum coherence above some threshold value not far below unity is a prerequisite for fault-tolerant quantum error correction (QEC). We study the initial dephasing of solid-state qubits in the independent-boson model, which describes well recent experiments on quantum dot (QD) excitons both in bulk and in substrates of reduced geometry such as nanotubes. Using explicit expressions for the exact coherence dynamics, a minimal QEC rate is identified in terms of error threshold, temperature, and qubit-environment coupling strength. This allows us to systematically study the benefit of a current trend towards substrates with reduced dimensions.

PACS. 03.65.Yz Decoherence; open systems; quantum statistical methods – 78.67.Hc Quantum dots – 63.20.kd Phonon-electron interactions

1 Introduction

Two-level systems with long-lived quantum coherence are candidate qubits, the units of quantum information [1]. Interactions between solid-state qubits and substrate phonons cause decoherence. It seems natural to fight decoherence by reducing the number of substrate degrees of freedom, by going from bulk to planar or linear geometries. In fact, QDs can nowadays be embedded in confined structures such as freestanding semiconductor membranes [2,3] or nanotubes and nanowires [4,5]. Such substrates may allow tailoring the phonon spectrum and, thus, controlling the qubit dephasing. However, it is not obvious whether fewer substrate dimensions do mean less decoherence.

It is interesting to compare photoluminescence measurements of single QDs in bulk environment [6–9] and in nanotubes [10,11]. In both cases, pure dephasing due to deformation-potential coupling to acoustic phonons is the dominant decoherence mechanism [12,13] since relaxation occurs on a much longer time scale. Using a Markovian master equation, i.e. approximating dephasing as exponential decay with a coherence time T_2, one finds $T_2 = \infty$ for bulk and a finite T_2 time for 1D substrates (details below); this would be an argument *against* reducing substrate dimensions. However, both in bulk and in reduced geometries, fast dephasing at short times has been observed as a broad background in spectra [6–9,11,14]. According to reference [11], it is this *non*-exponential decay that may hamper applications for quantum information processing (QIP) with 1D substrates. But are these really less ideal?

Future QIP devices will require built-in QEC, as some decoherence is inevitable. From the information-theoretical side come stringent requirements for fault-tolerant QEC: gate error levels ϵ should be less than 10^{-3} [15], a value that may be relaxed in the future. Usually assumptions such as local and Markovian decoherence go into the derivation of ϵ. One may criticize these [16,17] and go beyond them [18]. We start from the other end, with a given ϵ and a realistic qubit-bath model.

In this article, we study the minimal rate $\omega_{\rm qec}$ at which single-qubit errors should be corrected, requiring the coherence to stay above the threshold value $1-\epsilon$. The beautiful experiments on QDs in bulk (3D) [6,8,19] and on nanotube excitons (1D) [11] are well explained by the so-called independent-boson model, and we employ its generic version. We present analytical expressions for $\omega_{\rm qec}$ and for the exact coherence dynamics, with the substrate dimension as a free parameter, that reproduce the measured rich dynamics and lead to new predictions: How can parameters best be changed such that error correction is needed less frequently?

2 Model

To account for the coupling of the QD to quantized lattice vibrations, we follow references [7,20] and employ the independent-boson model with Hamiltonian

[a] e-mail: wubs@nbi.dk

$H = H_0 + H_{\rm qb}$, where $H_0 = \Delta\sigma_z/2 + \sum_{\mathbf{k}} \hbar\omega_{\mathbf{k}} b^\dagger_{\mathbf{k}} b_{\mathbf{k}}$ describes the uncoupled system of QD and bosons, with Pauli matrix σ_z for the qubit and creation and annihilation operators $b^{(\dagger)}_{\mathbf{k}}$ for phonons of mode $\mathbf{k}$. We focus on the dominant deformation-potential coupling to acoustic phonons with dispersion $\omega_{\mathbf{k}} = v_s|\mathbf{k}|$ where v_s denotes the sound velocity. The qubit-boson interaction

$$H_{\rm qb} = \hbar\sigma_z \sum_{\mathbf{k}} g_{\mathbf{k}}(b_{\mathbf{k}} + b^\dagger_{-\mathbf{k}}) \tag{1}$$

is characterized by microscopic couplings $g_{\mathbf{k}}$ proportional to $D_s\sqrt{|\mathbf{k}|/2\hbar\rho V v_s}$ in terms of a deformation potential D_s for the excitons, the mass density ρ and the volume V [7,14,21]. The more specialized model of references [7,11] takes different deformation potentials and confinement lengths for electrons and holes into account. As shown below, our simpler model is already accurate enough and has the major advantage that explicit expressions for the coherence decay can be obtained. The phonon bath gives rise to the spectral density $J(\omega) = \sum_{\mathbf{k}} |g_{\mathbf{k}}|^2 \delta(\omega - v_s|\mathbf{k}|)$ which for deformation-potential coupling and spherical QD symmetry with confinement length l_s has the form

$$J_s(\omega) = \alpha_s \omega^s \omega_{\rm c}^{1-s} \exp(-\omega/\omega_{\rm c}), \tag{2}$$

with cutoff frequency $\omega_{\rm c} = v_s/l_s$ and dimensionless coupling strength α_s.

3 Exact dynamics for arbitrary substrate dimension

Experimentally, a δ-like optical excitation pulse creates a coherent superposition of the ground state $|0\rangle$ (no exciton) and the one-exciton state $|1\rangle$. The exciton does not exist before the fast pulse, so it is safe to assume that the qubit and the phonon bath initially are in a direct-product state, with the phonons in a thermal state. After the initialization, the state of the qubit is determined by its interaction (1) with the acoustic phonons. Qubit populations do not change, but coherences ρ_{01} may decay by pure dephasing. We write $\rho_{01}(t) = \rho_{01}(0)c_s(t)$, and concentrate on the coherence function $c_s(t)$ in the following.

By solving the exact dynamics and tracing out the phonon bath, we find the explicit expression for the qubit coherence $c_s(t)$, i.e. the exciton polarization after a δ-like excitation pulse. In terms of the scaled temperature $\theta = k_{\rm B}T/\hbar\omega_{\rm c}$, the dynamics is given by $c_s(t) = \exp[-\lambda_s(t)]$, with the exponent

$$\lambda_s(t) = 8\alpha_s(-\theta)^{s-1}\left[F^{(s-1)}(\theta) - \mathrm{Re}\,F^{(s-1)}(\theta[1+i\omega_{\rm c}t])\right] + 4\alpha_s\Gamma(s-1)\left(\frac{\cos[(s-1)\arctan(\omega_{\rm c}t)]}{(1+\omega_{\rm c}^2t^2)^{(s-1)/2}} - 1\right), \tag{3}$$

where $\Gamma(z)$ denotes Euler's Gamma function, $F(z) = \log\Gamma(z)$ and its n-th derivative $F^{(n)}(z)$ which for positive n equals the Polygamma function $\Psi_{n-1}(z)$. Hereby we generalize previous results for qubit dephasing [7,17] to spectral densities with arbitrary $s = 1, 2, 3, \ldots$

We will now briefly discuss the qualitatively different dynamics for 3D, 2D, and 1D substrates, discuss the accuracy of our model, and present new analytical results, all based on equation (3), before comparing the error correction rates $\omega_{\rm qec}$ for the three geometries.

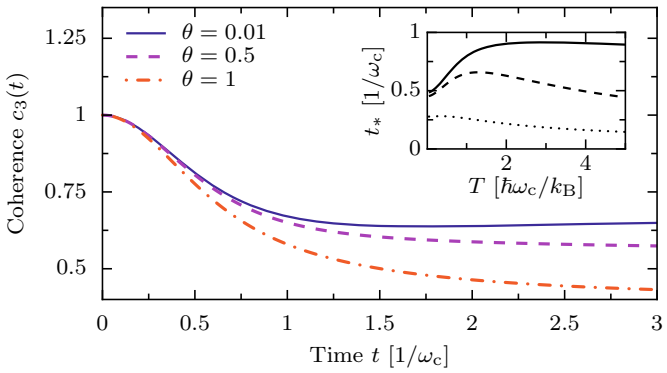

Fig. 1. (Color online) Time evolution of coherence for bulk structures with $s = 3$ at different scaled temperatures $\theta = k_{\rm B}T/\hbar\omega_{\rm c}$ with $\alpha_3 = 0.1$. Inset: non-monotonic temperature-dependence of the decay time t_* for different coupling strengths $\alpha_3 = 0.01$ (solid), 0.1 (dashed), and 0.8 (dotted). t_* is defined as the time at which the coherence has dropped "half-way" to $[1 + c_3(\infty)]/2$, see reference [19].

3.1 Three-dimensional substrates

Dephasing due to acoustic phonons in bulk geometries is described by equation (3) for $s = 3$ (for deformation-potential coupling, the parameter s equals the dimension of the substrate). While a Markovian master equation for our model would predict no decoherence at all, the exact dynamics in Figure 1 exhibits a fast initial decay of coherence, after which the coherence stabilizes to the final value

$$c_3(\infty) = \exp[-8\alpha_3(\theta^2\Psi_1(\theta) - 1/2)], \tag{4}$$

with zero-temperature limit $\exp(-4\alpha_3)$. Hence considerable initial decay may occur even at low temperatures, as the solid (blue) curve in Figure 1 illustrates. Using the parameters of references [7,9] for GaAs-based self-assembled QDs, we obtain the typical values $\alpha_3 = 0.8 \pm 0.3$ and $\omega_c = 5 \times 10^{12}$ s^{-1}, in close agreement with the experimental results of references [6,19]. For the exciton in the QD we find $l_3 = 10$ nm, a value in between the known confinement lengths of electron and hole wave functions. In reference [19] a decay time t_* was defined as the time at which half of the coherence that finally will get lost is lost. Theory and experiment agreed well on the point that t_* behaves non-monotonically as a function of temperature. In the inset of Figure 1, we find for our model similar non-monotonic behavior, another illustration that dephasing of real QDs is also well described by our generic model. Notice the short time scale of the decay, $t_* < \omega_c^{-1}$. There is monotonic dependence on other parameters as

well: t_* gets longer by making the QD larger, phonon velocity v_s slower, or the coupling α_3 smaller. As Figure 1 shows, the amount of coherence lost during short times is considerable for this realistic choice of parameters. If for QIP applications any phase errors beyond the percent level have to be corrected, then this should occur well within t_*.

Experimentally the coherence dynamics is usually inferred from absorption spectra. The Fourier transform of the highly non-exponential coherence dynamics in Figure 1 predicts a highly non-Lorentzian spectrum. Since $c_3(\infty) > 0$, the zero-phonon line at frequency $\Delta/\hbar$ is even a delta function, with weight $c_3(\infty)$ [12]. In practice this spectral line has a very narrow finite width, finite due to slow processes not described by the independent-boson model. However, with QIP in mind, we are more interested in the fast initial decay, which shows up as the broad background of the zero-phonon line.

3.2 Two-dimensional substrates

Let us briefly also consider dephasing in planar geometries. To our knowledge, experiments analogous to [11,19] with planar geometries have not yet been carried out. The exact dynamics is obtained by setting $s = 2$ in equation (3). Again a fast initial decay on a time scale ω_c^{-1} is found. The coherence $c_2(t)$ does not stabilize to a finite value, but vanishes algebraically $\propto 1/(\omega_c t)^{8\alpha_2\theta}$, leading to a nontrivially broadened zero-phonon line in the absorption spectrum.

3.3 One-dimensional substrates

For $s = 1$, the spectral density $J_s(\omega)$ becomes ohmic, i.e. linear in frequency up till the cutoff frequency ω_c. This describes dephasing due to acoustic phonons in 1D geometries such as nanotubes and nanowires, for which it is well known that the coherence dynamics strongly differs from the 3D case [11,14]. Detailed experiments have been performed only recently [11]. From equation (3) we find the exact analytical expression

$$\lambda_1(t) = 8\alpha_1\{\log\Gamma(\theta) - \log|\Gamma(\theta[1+i\omega_c t])| - \frac{1}{4}\log(1+\omega_c^2 t^2)\}. \quad (5)$$

For long times $t \gtrsim \max\{\omega_c^{-1}, \hbar/k_B T\}$, this gives

$$c_1(t) = \kappa(\alpha_1, \theta)\ \exp(-t/T_2), \quad (6)$$

i.e. exponential decay with coherence time $T_2 = \hbar/4\pi\alpha_1 k_B T$. This complete decay corresponds to a zero-phonon line with finite width [11,14]. Master equations would give the same T_2 time, but not the prefactor

$$\kappa(\alpha_1, \theta) = [2\pi\theta^{2\theta-1}/\Gamma^2(\theta)]^{4\alpha_1}, \quad (7)$$

by which the initial non-exponential decay remains noticeable also at long times. (See also the interesting discussion in Ref. [22], where another κ is found.) In the limit $\theta \ll 1$ we find $\kappa = (2\pi\theta)^{4\alpha_1}$. Dephasing cannot be reduced indefinitely by lowering the temperature. Rather, the duration of the non-exponential decay is increased. For the experiments in reference [11] with isolated single-wall nanotubes, we estimate $\alpha_1 = 0.1 \pm 0.05$ and $\omega_c = 20 \times 10^{12}$ s^{-1}. With temperatures ranging from 5 K to 32 K, i.e. θ between 0.033 and 0.21, κ assumes values between 0.49 and 0.92. Thus non-exponential dephasing is important in state-of-the-art 1D systems, the more so for lower temperatures.

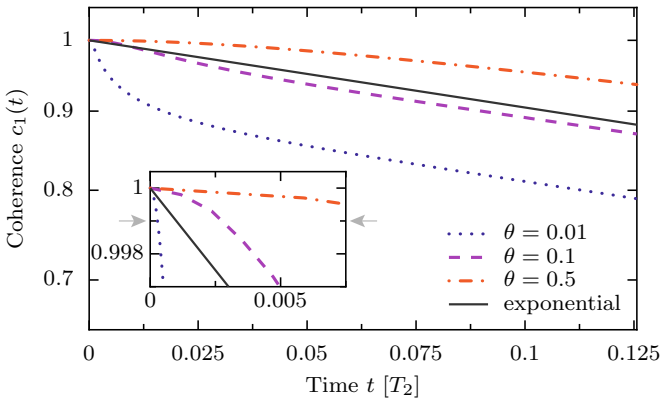

Fig. 2. (Color online) Exact coherence dynamics for a 1D environment with ohmic spectral density with coupling strength $\alpha_1 = 0.01$, for several scaled temperatures $\theta = k_B T/\hbar\omega_c$. The time-axis is scaled by θ. The solid line shows the approximated exponential decay as given by the T_2 time (see text). Inset: same as main figure, but on a shorter time scale. The arrows indicate an error threshold $\epsilon = 10^{-3}$.

Again, our main interest is the initial decay itself, rather than its effect at long times. For $\theta \leq 1$, the time scale of the non-exponential decay is $\hbar/k_B T$, in clear contrast to the temperature-independent t_* for bulk systems. Figure 2 shows the typical coherence dynamics of QDs on 1D substrates. We chose $\alpha_3 = 0.01$, an order of magnitude smaller than in the experiment of reference [11], but non-exponential decay would be important even then. The figure shows curves for three different temperatures, as well as their master-equation approximations $\exp(-t/T_2)$. The latter coincide due to scaling of the time axis. By contrast, the three exact curves do not coincide at all: the low-temperature curve ($\theta = 0.01$) is systematically lower and the high-temperature curve higher than their exponential-decay approximations. The inset of Figure 2 shows that when asked how long $c_1(t)$ manages to stay above 0.999, the exponential-decay curve may be too optimistic, too pessimistic, or accurate by chance.

4 Rate of quantum error correction

There is the danger of comparing apples and oranges when studying the effect of substrate dimensions. Fortunately in this respect, in state-of-the-art experiments both α_3 and α_1 turn out to be of order 10^{-1} (see above). For current and future experiments, it is therefore useful to depict the α_s-dependence of dephasing for all three geometries in the same range $\alpha_s \simeq 0.1$ and smaller.

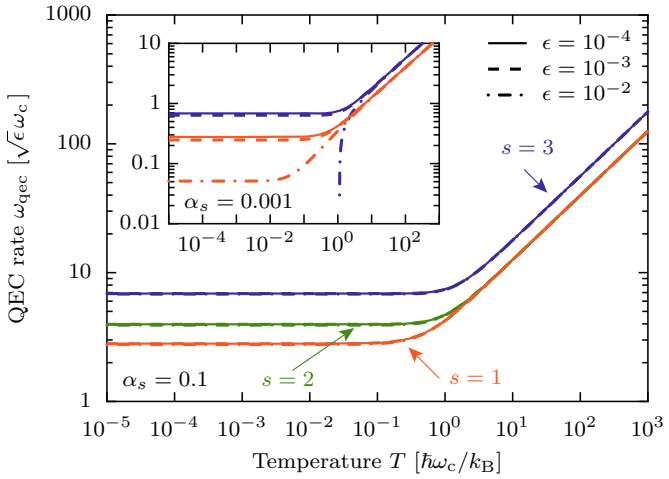

Fig. 3. (Color online) Temperature dependence of the quantum error correction rate $\omega_{\rm qec}$ for substrate geometries with spectral densities $J_s(\omega)$ with different s but equal couplings α_s, for several threshold values ϵ. In the main figure $\alpha_s = 0.1$, and $\alpha_s = 0.001$ in the inset, where case $s = 2$ is not shown. The y-axes are scaled by $\sqrt{\epsilon}$. Curves are based on equation (3).

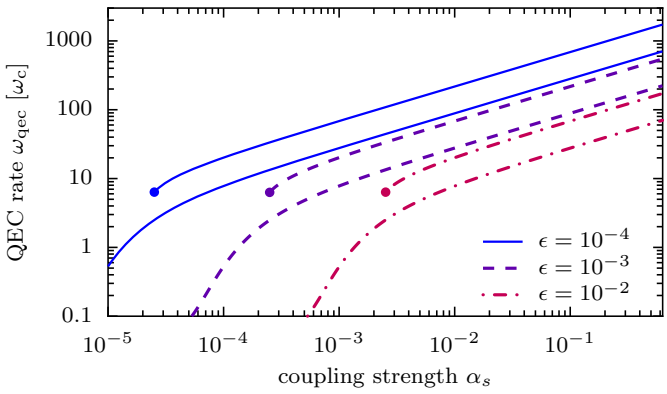

Fig. 4. (Color online) Quantum error correction rate $\omega_{\rm qec}$ as a function of coupling α_s, for several error thresholds ϵ. Curves were made using equation (3). For all three pairs of curves, $s = 1$ corresponds to the lower, and $s = 3$ to the upper curve. The curves for $s = 3$ stop at critical coupling strengths indicated by dots: for smaller α_3, the coherence $c_3(t)$ never decays below threshold. The temperature is $T = 0.01\hbar\omega_{\rm c}/k_{\rm B}$.

Let us now assume that phase errors have to be corrected if coherence drops from $c_s(0) = 1$ to $c_s(2\pi/\omega_{\rm qec}) = (1 - \epsilon)$ for some error threshold ϵ, i.e. from the exact dephasing dynamics (3) we identify the minimal rate $\omega_{\rm qec}$ at which phase errors have to be corrected in order to preserve coherence in an idle qubit. Reference [23] discusses how to correct phase errors. To be optimistic, we assume that in each step the error can be corrected perfectly and instantaneously. The central idea is that structures with lower rates $\omega_{\rm qec}$ are better suited for the implementation of quantum error correction.

In Figure 3 we compare $\omega_{\rm qec}$ as a function of temperature for bulk, planar, and linear substrate geometries. All couplings are $\alpha_s = 0.1$. Notice that $\omega_{\rm qec}$ on the vertical axis is scaled by $\sqrt{\epsilon}$. We find that the curves for the error correction tresholds $\epsilon = 10^{-4}, 10^{-3}$, and 10^{-2} overlap for all three geometries. Thus $\omega_{\rm qec}$ scales as $\sqrt{\epsilon}$, at least for current experimental couplings $\alpha_s = 0.1$ and $\epsilon \leq 10^{-2}$. Scaling with $\sqrt{\epsilon}$ only holds if the parabolic short-time approximation $c_s(t) \approx 1 - \eta_s t^2$ is still valid at the time that $c_s(t)$ assumes the threshold value $(1 - \epsilon)$. We find

$$\eta_s(\alpha_s, \theta) = 2\alpha_s[2(-\theta)^{s+1}\Psi_s(\theta) - s!], \qquad (8)$$

and for a small treshold ϵ, the error correction rate needs to be $\omega_{\rm qec} = 2\pi\sqrt{\eta_s/\epsilon}$. For $\alpha_s = 0.1$, the temperature dependence of η_s and hence of $\omega_{\rm qec}$ is completely negligible, even up to temperatures as high as $\hbar\omega_c/k_{\rm B}$. This corroborates that the first stage of pure dephasing is due to vacuum noise [17,24]. All rates $\omega_{\rm qec}$ corresponding to $\alpha_s = 0.1$ in Figure 3 are high and lie in the range between the cutoff $\omega_{\rm c}$ and the qubit frequency $\Delta/\hbar \simeq 10^{15}$ s^{-1}, since already the fast initial decay reaches the error threshold. However, this simple scaling breaks down for very weak coupling $\alpha_s = 0.001$, as shown in the inset of Figure 3, where the error correction rate depends on more than the initial parabolic decay. Figure 3 also shows that the rates for 1D are smaller than for 3D or 2D geometries, although by factors less than 10. Generally we find the central result that *linear substrate geometries like nanotubes and nanowires will perform best.*

It would be very challenging to implement a quantum error correction protocol for phase errors at rates as high as those shown in Figure 3. In our model, lower rates $\omega_{\rm qec}$ could be realized by reducing the cutoff frequency ω_c or the couplings α_s. Figure 4 shows the effect of the latter strategy. For the largest couplings $\alpha_s \simeq 0.1$, the message is as in Figure 3: given an error level ϵ, linear substrates have lower rates $\omega_{\rm qec}$ than planar or bulk substrates. As the α_s are decreased, this message is essentially unchanged, until suddenly for bulk substrates α_3 becomes so small that $c_3(\infty) > 1 - \epsilon$, i.e. the final coherence stabilizes above the error threshold. In that situation – which can not occur for 1D substrates – $\omega_{\rm qec}$ vanishes: error correction is not needed. State-of-the-art exciton qubits in QDs have couplings that are more than one order of magnitude larger than the largest critical coupling shown (i.e. for $\epsilon = 0.01$). Obviously $\omega_{\rm qec}$ would also become smaller if larger errors ϵ were allowed. The challenge is here to come up with QEC protocols that tolerate larger faults. All in all, Figure 4 shows that for fixed $\alpha_s = \alpha$ and ω_c, linear substrate geometries are to be preferred for their lower $\omega_{\rm qec}$, unless couplings can be substantially reduced.

5 Discussion and conclusions

Inspired by recent measurements [11,19], we have analyzed the first few percents of loss of quantum coherence of a solid-state exciton qubit on 3D, 2D, and 1D substrates. It is mainly this initial decoherence which is important for QIP applications when supplemented with fault-tolerant QEC. We proposed and focused on the important quantity

$\omega_{\rm qec}$, the minimal rate at which quantum errors have to be corrected. Its temperature dependence turned out to be negligible. For QD exciton qubits in a bulk substrate, the coherence may stabilize above the threshold, as for spin qubits [25], but corresponding couplings α_3 are currently not weak enough.

Let us return to our initial question: is it beneficial for QIP applications to reduce the dimensions of the substrate, as far as dephasing is concerned? From a master-equation perspective it is not, and worries about non-exponential decay were expressed especially for 1D structures [11]. We have presented analytical solutions of a generic but accurate independent-boson model to show how fast initial dephasing occurs for 1D, 2D, and 3D geometries alike, and identified the minimal rate at which single-qubit errors have to be corrected. In all cases the rates are high and fall in between the cutoff and the qubit frequency, which poses a challenge for QIP applications. However, we found that qubits on 1D substrates require the lowest error correction rates.

This work has been supported by the the DFG through SFB 631, by the German Excellence Initiative via "Nanosystems Initiative Munich (NIM)", and by the Niels Bohr International Academy.

References

1. M.A. Nielsen, I.L. Chuang, *Quantum Computing and Quantum Information* (Cambridge University Press, 2000)
2. E.M. Höhberger, T. Krämer, W. Wegscheider, R.H. Blick, Appl. Phys. Lett. **82**, 4160 (2003)
3. E.M. Weig et al., Phys. Rev. Lett. **92**, 046804 (2004)
4. S. Sapmaz, P. Jarillo-Herrero, L.P. Kouwenhoven, H.S.J. van der Zant, Semicond. Sci. Technol. **21**, S52 (2006)
5. M.T. Björk et al., Nano Lett. **4**, 1621 (2004)
6. P. Borri et al., Phys. Rev. Lett. **87**, 157401 (2001)
7. B. Krummheuer, V.M. Axt, T. Kuhn, Phys. Rev. B **65**, 195313 (2002)
8. P. Borri et al., Phys. Rev. B **71**, 115328 (2005)
9. B. Krummheuer et al., Phys. Rev. B **71**, 235329 (2005)
10. A. Högele, C. Galland, M. Winger, A. Imamoğlu, Phys. Rev. Lett. **100**, 217401 (2008)
11. C. Galland, A. Högele, H.E. Türeci, A. Imamoğlu, Phys. Rev. Lett. **101**, 067402 (2008)
12. C.B. Duke, G.D. Mahan, Phys. Rev. **139**, A1965 (1965)
13. T. Takagahara, Phys. Rev. Lett. **71**, 3577 (1993)
14. G. Lindwall, A. Wacker, C. Weber, A. Knorr, Phys. Rev. Lett. **99**, 087401 (2007)
15. P. Aliferis, D. Gottesman, J. Preskill, Quant. Inf. & Comput. **8**, 181 (2008)
16. R. Alicki, D.A. Lidar, P. Zanardi, Phys. Rev. A **73**, 052311 (2006)
17. R. Doll, M. Wubs, P. Hänggi, S. Kohler, Phys. Rev. B **76**, 045317 (2007); R. Doll, M. Wubs, P. Hänggi, S. Kohler, Europhys. Lett. **76**, 547 (2006)
18. B.M. Terhal, G. Burkard, Phys. Rev. A **71**, 012336 (2005)
19. A. Vagov et al., Phys. Rev. B **70**, 201305(R) (2004)
20. G.D. Mahan, *Many-Particle Physics*, 2nd edn. (Plenum Press, 1990)
21. T. Takagahara, Phys. Rev. B **60**, 2638 (1999)
22. F.K. Wilhelm, New J. Phys. **10**, 115011 (2008)
23. D.V. Averin, R. Fazio, JETP Lett. **78**, 664 (2003)
24. G.M. Palma, K.-A. Suominen, A.K. Ekert, Proc. R. Soc. London, Ser. A **452**, 567 (1996)
25. D. Mozyrsky, S. Kogan, V.N. Gorshkov, G.P. Berman, Phys. Rev. B **65**, 245213 (2002)